Original scientific papers UDK 678:669.14
DOI 10.7251/COMEN1901035M

GADOLINIUM SORPTION ON MULTI-WALLED CARBON NANOTUBES

Danijela Maksin[1], Marija Vukčević[2], Tatjana Đurkić[2], Ivana Stanišić[2], Tamara Bakić[3], Milena Radomirović[3], Antonije Onjia[2]*

[1] University of Belgrade, Vinča Institute of Nuclear Sciences, Belgrade, P.O. Box 522, Serbia,
[2] University of Belgrade, Faculty of Technology and Metallurgy, Belgrade, Karnegijeva 4, Serbia
[3] University of Belgrade, Innovation Center, Faculty of Technology and Metallurgy, Belgrade, Karnegijeva 4, Serbia

Abstract: Rare earth metals are deemed to be the materials of future due to their numerous applications including medical diagnostics, nuclear facilities, petroleum industry, etc. In this paper, multi-walled carbon nanotubes, which possess unique physicochemical properties, were evaluated as sorbents for lanthanoid gadolinium from aqueous solutions. The pH-dependent sorption behavior of Gd was studied in the pH range from 3 to 11 at room temperature (298 K). Equilibrium data over a range of initial Gd concentrations of 5−50 mg L^{-1} was analyzed with Langmuir, Freundlich and Redlich-Peterson models. Sorption kinetics was fitted with the pseudo-first-order, the pseudo-second-order and fractional power kinetic models.

Keywords: gadolinium; multi-walled carbon nanotubes; sorption.

1. INTRODUCTION

Carbon nanostructure materials of diverse chemical compositions, produced as nanoparticles, nanowires or nanotubes, are unique due to their mechanical, electrical, optical, catalytic, magnetic and photonic characteristics and extremely large surface area [1,2]. The possibilities of technical use of carbon nanomaterials seem to be unlimited, which inevitably brought about their exploitation for environmental purposes and their rapid release into the ecosystem [3,4]. The large specific surface area, the outstanding thermal and chemical stabilities and the latest advances in large-scale synthesis render carbon nanostructures as promising materials for detection and separation of an array of organic compounds, metal ions and their complexes [1,3,5,6]. Especially, carbon nanotubes (CNTs) have been termed 'materials of the 21st century' [7] due to their distinctive properties which depend on the diameter and length of the nanotubes, and their morphology [8].

CNTs surface functional groups and hydrophobic surfaces can account for strong interactions with heavy metal ions and organic compounds, respectively, so their presence in the environment affects the physicochemical behavior of common pollutants [3].

Comparing to other carbon-based adsorptive materials, CNTs offer chemically inert surfaces for physisorption with high specific surface areas which measure up to those of activated carbons. Among other factors, the adsorption properties of CNTs depend on contribution of individual adsorption sites [9]. For as produced CNTs, where both ends are generally closed, the possible sites in CNT bundles where the adsorption takes place are the grooves, the outer surface sites, and large-diameter stacking-defect induced interstitial channels [10,11]. The phenomenon of aggregation of CNTs in aqueous solutions limits the accessible sites for binding with pollutants in liquid. Changing surface chemistry via diverse chemical treatments to improve dispersion of CNTs in solution can significantly enhance the interaction of CNTs with pollutants and thus their adsorption capacity and their extraction efficiency, which are strongly pH-dependent [12,13]. One of the major downsides of widespread acid-oxidation methods apply is CNT fragmentation and the production of defects in the graphitic network [14].

* Corresponding author: dmaksin@vinca.rs

Fragmentation is also caused by the high ultrasonic power typically utilized to disperse CNT agglomerates during oxidation [15]. Hence, a compromise needs to be found between functionalization parameters and CNT damage. By adjusting the modification conditions, and thus quantity and nature of surface oxygen groups, the wettability of MWCNT surfaces can be altered and more hydrophilic MWCNTs can be the outcome. Conversely, functional groups may increase diffusion resistance and hinder the access of sorbate molecules [13].

Rare earth elements (REEs) or rare earth metals (REMs), as defined by IUPAC, stand for a group of 17 chemically and physically similar transient metals (scandium, yttrium and further 15 elements called lanthanides ranging from the most abundant cerium and lanthanum to the less frequent lutetium), naturally more abundant than their name would imply [16,17]. They exhibit low solubility and mobility in soil and are usually in the +3 valence state in oxic and anoxic conditions [16].

REEs are recognized as materials of the future due to their importance and applications [18]. Due to the distinctive magnetic, electric and optical properties, REEs and their compounds apply in many kinds of industrial products [16]. World demand for REE reached 185 000 tons in the year of 2015 [19]. A drastic rise has been observed in the last three decades, mainly due to the transition to green, low-carbon economy where they have an essential role in an increasing number of energy technologies such as rechargeable batteries (La), wind turbines (Sm, Dy, Pr, Nd), lamp phosphors (La, Gd, Tb, Eu, Yb), as car catalysts (Ce) and hybrid vehicles (Dy, La, Nd) [20], magnetic alloys (Nd, Dy, Tb, Pr), catalysts for petroleum refining, high-refractive index low-dispersion optical glasses [21,22], fertilizers (Pr, Nd, Sm, Tb, Dy, Er) [23], etc.

The gadolinium compounds are also used in nuclear medicine as magnetic resonance imaging contrast reagents [24] and Gd itself is a “neutron poison”, with its most effective isotope Gd-157 having the highest neutron cross-section among the stable isotopes of 254 000 barns for thermal neutrons. [25] Gadolinium is used in CANDU® reactors to suppress excess reactivity or as an emergency shut-down measure [26]. Gd^{3+} is identified as the most paramagnetic ion, due to its electronic structure (its $4f^7$ subshell is intact in its ionic state) [27] About 1.0 g of Gd is applied for one enhanced MRI scan in the form of commercially available contrast agents [28]. Thus, a large quantity of anthropogenic Gd is discharged into our ecosystem every day and commonly used wastewater treatment technologies have not been successful in its elimination owing to its good water solubility and tendency to form stable complexes [18].

European Union Commission and the US Department of Energy regard REEs as the most critical raw materials with higher supply risk [29]. However, it was stated that only approximately 3% of the REEs were recycled in 2011 [30].

Since REEs bioaccumulate along the food chain, constant exposure to low concentrations of REEs could cause adverse health effects [31]. A number of deleterious effects due to occupational and environmental exposure to REEs have been registered [32,33], albeit no incidence of intoxication due to the intake of REEs through the food chain has thus far been reported. Hence, the monitoring of REEs in biological and environmental samples is of great significance. [34].

A growing concern about the possible toxicity of Gd to the living organisms due to its impact on the biochemistry of calcium and related cellular processes exists [35]. Several Gd chelate species were detected in environmental waters, but up to now, little is known about the bioavailability and transport of Gd species into biological systems [36,37]. It was demonstrated that free gadolinium is absorbed by various plants [38] and that the uptake of metal ions can be increased by chelation [39].

Toxicity of the free metal ions of lanthanides is lowered substantially via complexing with EDTA or DTPA [27]. The stability of Fe^{3+}-EDTA greater than EDTA chelated Gd^{3+}, so there is a possibility of conversion of nontoxic complexed Gd from MRI to noncomplexed and toxic Gd species, as Fe-(III)-salts are used during the flocculation within the drinking water purification process [40]. Both Zn^{2+} and Cu^{2+} are found in wastewater and reportedly these two cations react with $Gd(DTPA)^{2-}$ [41].

At the moment, China generates more than 90% of the global REE supply, so mining companies in the rest of the world are actively searching for new exploitable REE deposits and old mines are being reopened, but many countries will have to rely on recycling of REEs from pre-consumer scrap, industrial residues and REE-containing End-of-Life products, bearing in mind the so-called “balance problem” [22].

Multi-walled carbon nanotubes (MWCNTs) are chosen over single-walled carbon nanotubes (SWCNTs) for adsorption seeing that the presence of concentric graphene sheets improves the interaction with the analytes [42].

2. EXPERIMENTAL

2.1. Materials and methods

All chemicals were analytical grade products and used as received.

Gadolinium(III) 500 mg L^{-1} stock solution was prepared by dissolving analytical grade $GdCl_3 \cdot 6H_2O$ (99% titration, Sigma-Aldrich, USA**)** in 3% HNO_3 solution in deionized water (Milli-Q Millipore, 18 $M\Omega cm^{-1}$ conductivity) in order to avoid hydrolysis. The solution was further diluted to the required concentrations before the experiments.

Commercial multi-walled carbon nanotubes with the following characteristics: an average external diameter of 6–9 nm, the length of 5 μm, the number of walls 3–6, and 95% of carbon (Sigma-Aldrich, USA), were used for Gd(III) sorption experiments in their pristine state.

The concentrations of Gd(III) in filtrate solutions were analyzed by inductively coupled plasma optical emission spectrometry (ICP-OES, Thermo Scientific CAP 6000). Standard statistical methods were utilized to calculate the mean values and standard deviations for each set of data. All measurements were carried out in triplicate or more if necessary. Relative standard deviations were less than or equal to 5%.

2.2. Sorption procedures

All sorption experiments were conducted at room temperature (298 K), using the batch method. The ratio of solid sorbents to sorbate solutions was maintained at 0.5 g L^{-1}. The suspensions were mounted on shaker which was operated at agitation speeds (AS) in the range of 150-175 rpm. The stirring rates were chosen in order for MWCNTs to be homogeneously dispersed in the solutions.

After the suspensions were shaken for predetermined time intervals, the appropriate aliquots were diluted with deionized water and filtered through 0.45-μm membrane syringe filters.

To investigate the influence of the pH on sorption efficiency, 0.025 g of MWCNTs was introduced into 0.050 L^{-1} solution containing initial concentration of 10 mg Gd(III) L^{-1}. The pH values of the solutions were adjusted to 3.0 - 11.0 with 0.1M HNO_3 or 0.1M KOH.

Sorption kinetics experiments were carried out next to estimate the equilibrium time and rate constants. The initial Gd(III) concentrations were 5, 10 and 25 mg L^{-1} at optimum pH which allowed the exclusion of precipitation. The process appeared to be fast.

Equilibrium adsorption isotherm experiments were conducted over a range of initial Gd(III) concentrations from 5 to 50 mg L^{-1}, by agitating 20 ml of gadolinium (III) solution and 10 mg of MWCNTs The selection of contact time of 24 h was to assure the attainment of sorption equilibrium.

The amount of metal ions sorbed onto the unit mass of MWCNTs (sorption capacity, mg g^{-1}) at time t (min) was calculated using the following equation:

$$Q_t = \frac{(C_0 - C_t) \cdot V}{m} \quad (1)$$

where C_0 and C_t are the initial Gd concentation and Gd concentration after treatment for a certain period of time (mg L^{-1}), respectively, V is the volume of the aqueous phase (L) and m is the amount of MWCNTs used for the experiment (g).

Removal efficiency is given by the following equation:

$$RE(\%) = \frac{C_0 - C_e}{C_0} \cdot 100 \quad (2)$$

where C_e is the equilibrium Gd(III) concentration in solution (mg L^{-1}).

3. RESULTS AND DISCUSSION

3.1. Effect of pH on Gd(III) sorption by MWCNTs

The mechanisms of heavy metal ion adsorption on CNTs are very complicated and appear attributable to physical adsorption, electrostatic attraction, precipitation and chemical interaction between the heavy metal ions and the surface functional groups of CNTs **[**3**].**

Several factors, such as surface charge, speciation of heavy metal ions in solution and experimental conditions, affect the adsorption of heavy metal ions on CNTs, which leads to a dependence of the adsorbed amount on the point of zero charge of CNTs (pH_{PZC}) [3]. The properties of CNTs and the speciation of heavy metal ions are the two factors which have the greatest influence on the adsorption of metal ions on CNTs, The pH value plays an important role with respect to the sorption of metal ions on CNTs because the surface charge depends on the acidity of the surrounding electrolyte [1]. The pH_{PZC} of as-produced CNTs is in the range of pH 4–6 [43,44].

In the study by Gao at al. [45], it was demonstrated that for Ni^{2+}(aq), Cd^{2+}(aq) and Zn^{2+}(aq), all species were removed from solution at pH > 6 and suggested that particularly in the basic

pH range, deposition played the pivotal role in metallic ion removal [46].

Mohan et Sing [47] have shown that in the case of Cd(II) and Zn(II), at initial pH ≥ 8.0, the removal happens by adsorption as well as precipitation i.e. the hydroxide ions from the solution form insoluble complexes with metal ions. Gadolinium has a coordination number of 6-9 (even 10 for some compounds) and forms mixed aqua-hydroxo complexes $Gd(OH)_x(H_2O)_y^{+3-x}$ in neutral and basic solutions. $GdCl_3$ only remains in its "free" ionic form at pH ≤ 5 [48]. Above this pH, it is expected that insoluble hydroxide colloid would quickly appear. Mohan et Sing [47] observed that pH_{fin} in the acid range increased with the increasing pH_{in}, suggesting the occurrence of simultaneous neutralization and sorption processes, and at pH_{in} higher than 6.0, the pH_{fin} became relatively constant. We noticed a similar trend in our study. In view of the information, Mohan et Sing [47] chose the optimum initial pH of 4.5, to correlate the removal with the adsorption process.

It was ascertained in our previous work [13] that the BET surface of the untreated MWCNTs is equal to 252.1 m^2 g^{-1} with the average pore radius of 14.98 nm. It was also established by means of temperature programmed desorption that the surface groups present include lactones, carboxylic anhydrides, phenols, ethers, carbonyls and quinones.

Figure 1. shows the dependence of the removal percentage of Gd(III) on the initial pH value:

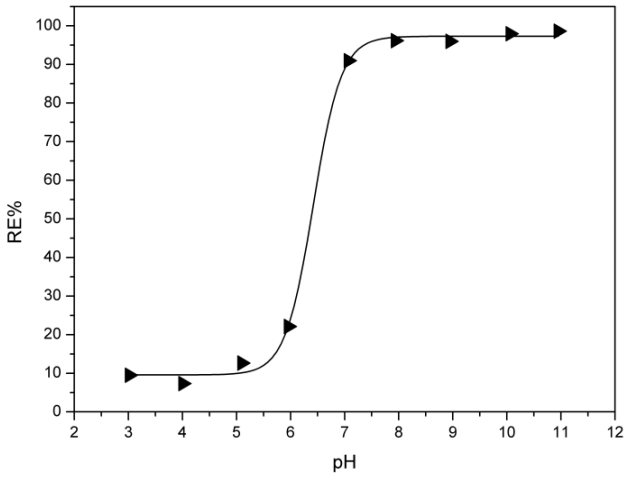

Figure 1. The effect of pH on Gd(III) sorption by MWCNTs (C_0 = 10 mg L^{-1}, T = 298 K, AS = 175 rpm, C_s = 0.5 g L^{-1})

An abrupt discontinuity can be seen in the graph between pH 6 and 7, that can be attributed to some of the issues stated above. Our data indicated that the most prudent course of action was to select the pH range of 5-5.5 for further experiments, in order to exclude any concurrent precipitation with adsorption.

3.2. Gd(III) sorption kinetics and kinetic modeling

Concentration-time profiles are presented in Figures 2.(a) and (b), and it is shown in all cases that Gd(III) sorption by MWCNTs is a single continuous curve which reaches saturation relatively quickly after approximately 60 min or sooner, indicating that the process is fast. The choice of different agitation speeds (150−175) was for the purpose of preliminary assessment of how small differences in degree of mixing influence sorption capacity of pristine MWCNTs. As expected, a positive correlation is noted.

Kinetic data were treated with the fractional power model, the pseudo-first-order and the pseudo-second-order kinetic models [48]. The fractional power function model is a modified form of the Freundlich equation; its linear form is given in equation (3):

$$\ln Q_t = \ln a + b \ln t \tag{3}$$

where *a* and *b* are constants with *b* < 1. By definition, the function *ab* which is a constant denotes the specific sorption rate when *t* = 1 [48].

Perhaps the earliest recognized and one of the most commonly used kinetic equations to date for the sorption of a solute from a liquid solution is Lagergren's equation or the pseudo-first order equation [48]:

$$\log\left(Q_{eq} - Q_t\right) = \log Q_{eq} - \frac{\left(k_1 t\right)}{2.303} \tag{4}$$

where k_1 is the rate constant of pseudo-first-order sorption (min^{-1}), Q_{eq} is the amount of sorbed gadolinium (mg g^{-1}) at equilibrium. A plot of $\log\left(Q_{eq} - Q_t\right)$ vs. *t* should give a straight line to confirm the applicability of the kinetic model. If the sorption process is truly the first-order process, $\log(Q_{eq})$ should be equivalent to the intercept of a plot $\log(Q_{eq} - Q_t)$ vs. t.

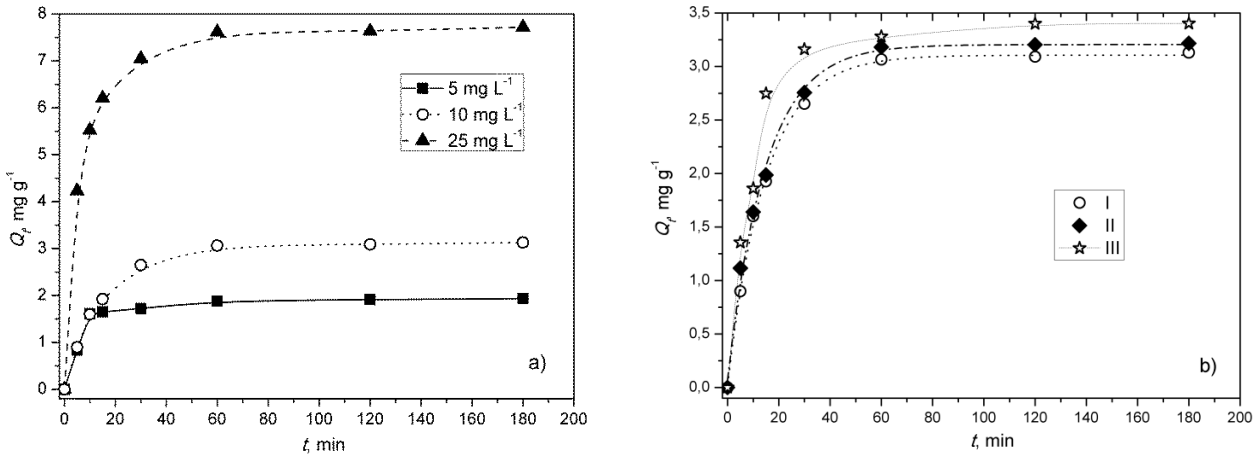

Figure 2. Concentration-time profiles for Gd(III) sorption by MWCNTs for (a) for various Cr(VI) initial concentrations (T = 298 K, pH = 5.0, AS = 150 rpm, C_s = 0.5 g L^{-1}) and (b) C_o=10 mg L^{-1}: I – pH =5.0, AS = 150 rpm; II - pH =5.0, AS = 175 rpm; III - pH =5.5, AS = 175 rpm (T = 298 K, C_s = 0.5 g L^{-1})

The pseudo-first order expression is more often than not able to describe kinetic data as well as the pseudo second order equation [49]. The pseudo-second-order rate equation is used to describe chemisorption involving the sharing or exchange of electrons between the sorbent and sorbate as covalent forces and ion exchange [50], quite often in its linear form [48]:

$$\frac{t}{Q_t} = \frac{1}{k_2 Q_{eq}^{\ 2}} + \frac{1}{Q_{eq}} t \tag{5}$$

where k_2 (mg^{-1}g^{-1}min^{-1}) is the rate constant of the pseudo-second order sorption. A plot of t/Q_t vs. t should give a linear relationship for the second-order kinetics. Furthermore, the initial sorption rate h (mg g^{-1} min^{-1}) of the pseudo-second order reaction can be determined using the following equation:

$$h = k_2 Q_{eq}^2 \tag{6}$$

The pseudo-second-order equation has no problem of designating an effective adsorption capacity which can be determined, along with the rate constant for pseudo-second-order and the initial adsorption rate, from the equation without knowing any parameters beforehand [51].

Kinetic parameters and the coefficients of determination, R^2, as well as the sorption half-time ($t_{1/2}$) are given in Tables 1, 2 and 3. As an illustration, plots $\log(Q_{eq} - Q_t)$ vs. t (pseudo-first order), t/Q_t vs. t (pseudo-second order) and ln Q_t vs. ln t (fractional power order) for Gd(III) sorption by MWCNTs were shown in Figures 3, 4 and 5:

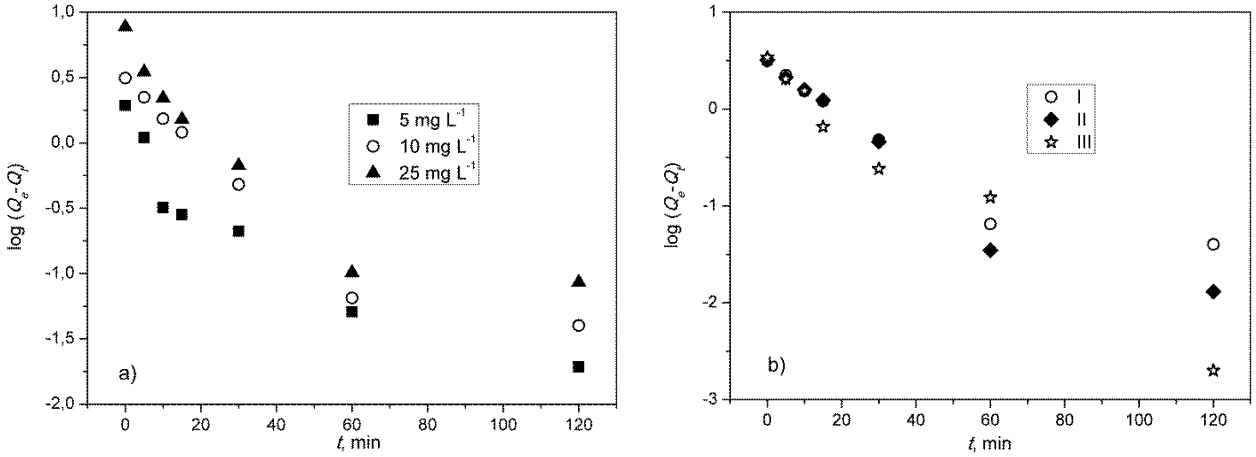

Figure 3. Pseudo-first order kinetics of Gd(III) uptake by MWCNTs for (a) various Cr(VI) initial concentrations (T = 298 K, pH = 5.0, AS = 150 rpm, C_s = 0.5 g L^{-1}) and (b) C_o=10 mg L^{-1}: I – pH =5.0, AS = 150 rpm; II - pH =5.0, AS = 175 rpm; III - pH =5.5, AS = 175 rpm (T = 298 K, C_s = 0.5 g L^{-1})

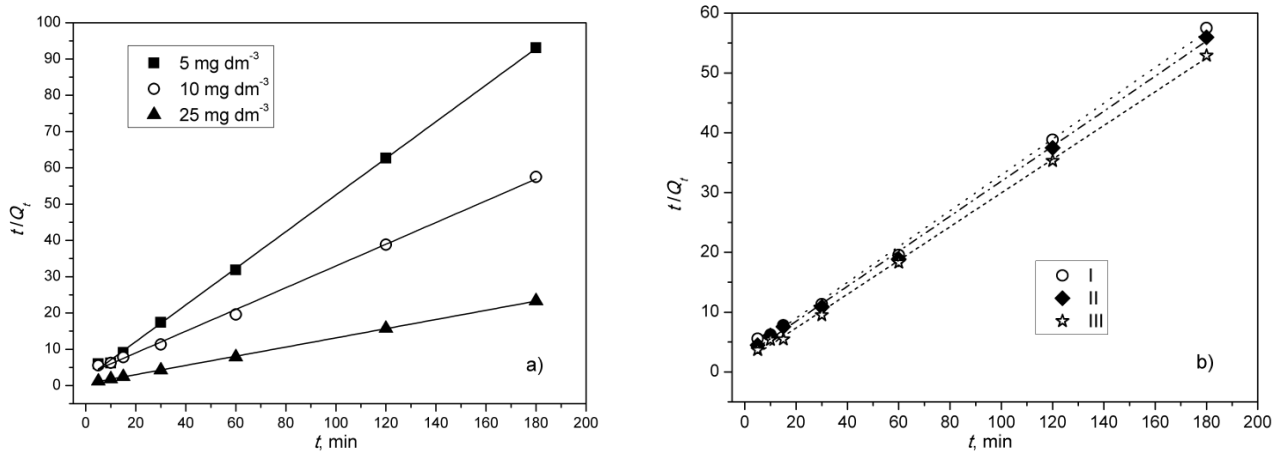

Figure 4. Pseudo-second order kinetics of Gd(III) uptake by MWCNTs for (a) various Cr(VI) initial concentrations (T = 298 K, pH = 5.0, AS = 150 rpm, C_s = 0.5 g L^{-1}) and (b) C_o=10 mg L^{-1}: I – pH =5.0, AS = 150 rpm; II - pH =5.0, AS = 175 rpm; III - pH =5.5, AS = 175 rpm (T = 298 K, C_s = 0.5 g L^{-1})

Table 1. Kinetic data for Gd(III) sorption on MWCNTs calculated from the pseudo-first and pseudo-second order models for various Cr(VI) initial concentrations (T = 298 K, pH = 5.0, AS = 150 rpm, C_s = 0.5 g L^{-1}).

Parameters	Experimental data		Pseudo-first order kinetics			Pseudo-second order kinetics			
C_0, mg L^{-1}	$t_{1/2}$, min	$Q_{e\,exp}$, mg g^{-1}	k_1, min^{-1}	Q_e, mg g^{-1}	R^2	k_2, g mg^{-1} min^{-1}	h, mg g^{-1} min^{-1}	Q_e, mg g^{-1}	R^2
5	6	1.94	0.0346	0.770	0.850	0.126	0.496	1.980	0.999
10	10	3.13	0.0381	2.045	0.883	0.030	0.333	3.339	0.998
25	5.5	7.72	0.0674	5.199	0.977	0.033	2.063	7.896	0.999

Table 2. Kinetic data for Gd(III) sorption on MWCNTs calculated from the pseudo-first and the pseudo-second order models for C_o=10 mg L^{-1}(T = 298 K, C_s = 0.5 g L^{-1}).

pH / AS, rpm	Experimental data		Pseudo-first order kinetics			Pseudo-second order kinetics			
	$t_{1/2}$, min	$Q_{e\,exp}$, mg g^{-1}	k_1, min^{-1}	Q_e, mg g^{-1}	R^2	k_2, g mg^{-1} min^{-1}	h, mg g^{-1} min^{-1}	Q_e, mg g^{-1}	R^2
5 / 150	10	3.13	0.0381	2.045	0.883	0.0298	0.333	3.339	0.998
5 / 175	9.5	3.22	0.0632	3.057	0.996	0.0328	0.382	3.415	0.999
5.5 / 175	8	3.40	0.0586	2.451	0.976	0.0465	0.584	3.543	0.999

Table 3. Kinetic parameters for Gd(III) sorption on MWCNTs calculated from the fractional power model for various Cr(VI) initial concentrations (T = 298 K, pH = 5.0, AS = 150 rpm, C_s = 0.5 g L^{-1}) and for C_o=10 mg L^{-1}(T = 298 K, C_s = 0.5 g L^{-1})..

C_0, mg L^{-1}	5	10	25	pH	5	5	5.5
a	0.878	0.711	3.781	AS, rpm	150	175	175
b	0.174	0.322	0.155	*a*	0.711	0.840	1.147
R^2	0.612	0.837	0.838	*b*	0.322	0.291	0.239
				R^2	0.838	0.873	0.774

Since the coefficients of determination for the pseudo-second-order kinetic model were higher than the corresponding values for the pseudo-first-order kinetic model, the pseudo-second-order kinetics model appears to be more adequate for description of the Gd(III) sorption by MWCNTs process. A further indication of this was that the experimentally achieved values for the equilibrium sorption capacities showed significantly better agreement with the calculated values from the pseudo-second-order model than those from the pseudo-first-order model. This indicated that the sorption rate is

controlled by both sorbent capacity and sorbate concentration. The initial sorption rate, *h*, generally increases with an increase in the initial Gd(III) concentration and the AS due to improved mass transfer.

Both pseudo-first-order and fractional power models failed to adequately represent experimental data over the whole duration of the experiment, and R^2 values for fractional power order were less than or equal to 0.838, showing especially poor correlation.

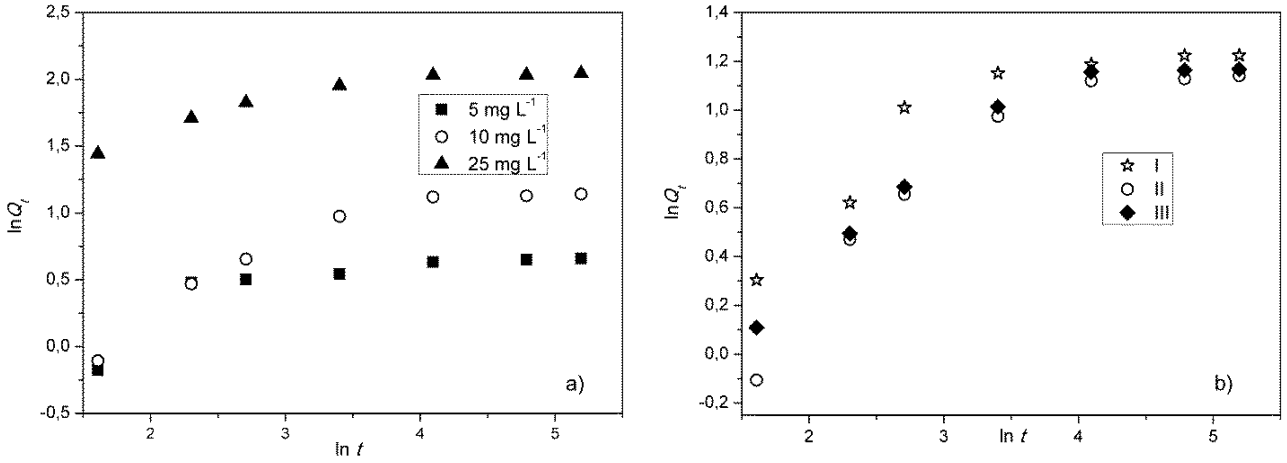

Figure 5. Fractional power model kinetics of Gd(III) uptake by MWCNTs for (a) various Cr(VI) initial concentrations (T = 298 K, pH = 5.0, AS = 150 rpm, C_s = 0.5 g L^{-1}) and (b) C_o=10 mg L^{-1}: I – pH =5.0, AS = 150 rpm; II - pH =5.0, AS = 175 rpm; III - pH =5.5, AS = 175 rpm (T = 298 K, C_s = 0.5 g L^{-1})

3.3. Equilibrium sorption of Gd(III) by MWCNTs and isotherm models

Sorption equilibrium and sorption kinetics supply essential physicochemical data for estimating the applicability of a sorption process as a unit operation [52]. An isotherm equation, whose parameters express the surface properties and affinity of the sorbent at a fixed temperature and pH, is an especially convenient way to assess the variation of sorption with a concentration of sorbate. It relates Gd(III) uptake per unit mass of MWCNTs (Q_e, mg g^{-1}) to the equilibrium sorbate concentration in the bulk liquid phase (C_e, mg L^{-1}) (see Figure 6.(a)) [53].

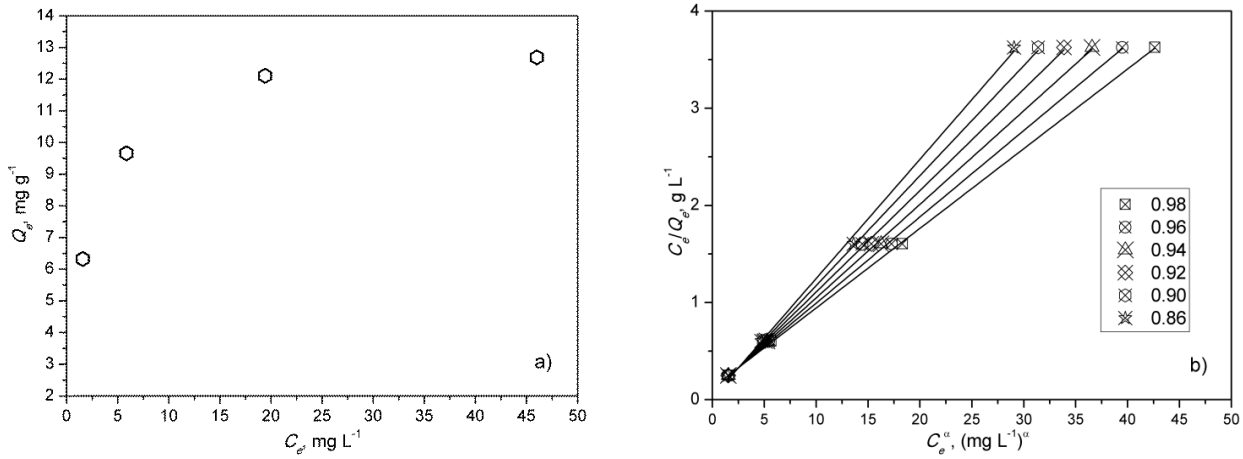

Figure 6.(a) Adsorption isotherm of Gd(III) sorption by MWCNTs (pH = 5.5, T = 298 K, AS = 175 rpm, C_s = 0.5 g L^{-1}) and (b) Redlich-Peterson isotherm for the sorption of Gd(III) by MWCNTs

The equilibrium adsorption data presented in Figure 6.(a) were fitted with Langmuir, Freundlich and Redlich Peterson equations (Table 5) in order to establish the isotherm model that is the most suitable to illustrate the acquired results. The Langmuir sorption isotherm predicts monolayer sorption at specific homogenous sites within the structurally homogeneous sorbent; all sorption sites are identical and energetically equivalent [54, 55]. Theoretically, the sorbent has a limited capacity for the sorbate and no sorption can take place after attaining a saturation

value. The linearized expression of the Langmuir isotherm model is given as:

$$\frac{C_e}{Q_e} = \frac{1}{Q_{\max} K_L} + \frac{C_e}{Q_{\max}} \quad (7)$$

where: Q_{max} is the monolayer capacity of the adsorbent (mg g^{-1}) and K_L is the Langmuir adsorption constant associated to the affinity of binding sites (L mg^{-1}). The key characteristics of this model can be expressed in terms of a dimensionless constant called Langmuir equilibrium parameter or separation factor R_L:

$$R_L = \frac{1}{1 + K_L C_i} \quad (8)$$

The value of R_L shows the type of the isotherm either to be unfavorable ($R_L > 1$), linear ($R_L = 1$), favorable ($0 < R_L < 1$) or irreversible ($R_L = 0$).

The Freundlich isotherm is an empirical model which presumes that reversible multilayer sorption occurs at a heterogeneous surface. The linear form of the Freundlich equation [56] is as follows:

$$\ln Q_e = \ln K_F + \frac{1}{n} \ln C_e \quad (9)$$

where K_F (dm^3 g^{-1}) and n are the Freundlich adsorption constants characteristic for the system.

The value of K_F is related to the degree of adsorption. Higher K_F values indicate a higher affinity for the investigated adsorbent. The Freundlich constant or heterogeneity factor ($1/n$) is also a measure of the departure of the sorption process from linearity when n=1. If the value of $1/n$ is smaller than 1, then the sorption capacity is enhanced and new sorption sites appear (favorable sorption). When the value of $1/n$ is larger than 1, the adsorption bond becomes weak; sorption is unfavorable which leads to a reduced sorption capacity [57].

The exponential linear form of the Redlich-Peterson isotherm model is given in the following form [58]:

$$\frac{C_e}{Q_e} = \frac{1}{b_{RP} Q'_{mon}} + \left(\frac{1}{Q'_{mon}}\right) C_e^{\alpha} \quad (10)$$

By trial and error, an optimum line for α is adopted. When α = 1, it is the same as the Langmuir isotherm equation. When $1/b_{RP}Q'_{mon}$ = 0, it is the same as the Freundlich isotherm equation. The plots of C_e/Q_e vs. Q_e are given in Figure 6.(b).

To provide a more extensive concentration range, the three-parameter Redlich-Peterson model has a linear dependence on concentration in the numerator and an exponential function in the denominator. The mechanism of adsorption is assumed to be a hybrid and it can be applied either in homogeneous or heterogeneous systems due to its adaptability [59].

Table 5. Calculated model constants and coefficients of determination

Langmuir		Freundlich		Redlich-Peterson	
Q_{max}, mg g^{-1}	13.21	n	4.771	α = 0.98	
K_L, L^{-1} g^{-1}	526	$1/n$	0.210	b_{RP}, m^2 g^{-1}	0.655
R_L	0.000364	K_F,(mg g^{-1})/(mg L^{-1})$^{1/n}$	6.133	Q_{mon}, mg g^{-1}	12.20
R^2	0.999912	R^2	0.932291	R^2	0.999883
				α = 0.96	
				b_{RP}, m^2 g^{-1}	11.25
				Q_{mon}, mg g^{-1}	0.838
				R^2	0.999770
				α = 0.94	
				b_{RP}, m^2 g^{-1}	1.117
				Q_{mon}, mg g^{-1}	10.38
				R^2	0.999569
				α = 0.92	
				b_{RP}, m^2 g^{-1}	1.595
				Q_{mon}, mg g^{-1}	9.58
				R^2	0.999276
				α = 0.90	
				b_{RP}, m^2 g^{-1}	2.585
				Q_{mon}, mg g^{-1}	8.83
				R^2	0.998889
				α = 0.88	
				b_{RP}, m^2 g^{-1}	5.846
				Q_{mon}, mg g^{-1}	8.15
				R^2	0.998403

The analysis of the equilibrium data with isotherm models showed that Gd sorption on MWCNTs adheres to Langmuir model, judging by the calculated coefficient of determination values, although $R^2 \geq 0.999$ for Redlich-Peterson model in the α range of 0.90-0.98 was attained as well.

To the best our knowledge, there are no published reports at this time of noncomplexed Gd sorption on pristine CNTs.

4. CONCLUSION

The capacity of as-produced MWCNTs for Gd(III) sorption was tested with respect to pH, time, agitation regime and initial concentration. The pristine MWCNTs showed affinity for Gd(III) sorption and the removal efficiency was strongly pH dependent with two distinct plateaus: the minimum of around 10% at pH < 6.0 and the maximum of close to 100% at pH ≥ 7.0. The resulting quantity of bound gadolinium at high pH values is due to a mixed process of adsorption and precipitation. The time-course data for sorption of Gd(III) by MWCNTs at pH 5.0−5.5 obeyed the pseudo-second-order kinetic model under all experimental conditions, proposing that the sorption rate is controlled by both sorbent capacity and sorbate concentration. The removal process was quite fast, with the maximum experimental capacity attained in 60 min. The isotherm data is best fitted with Langmuir model indicating homogeneous distribution of active sites on the MWCNTs and monolayer adsorption. The maximum monolayer sorption capacity at pH 5.5 and 298 K was found to be 13.21 mg g^{-1}. The results of this study are a promising starting point for further research into sorption of REEs by MWCNTs (pristine and modified), including desorption of bound metal species of interest and regeneration of sorbent.

5. ACKNOWLEDGEMENT

This work was supported by the Ministry of Education, Science and Technological Development of Serbia (Projects III43009, ON172007 and III45006).

6. LITERATURE

[1] K. Pyrzynska, *Carbon nanostructures for separation, preconcentration and speciation of metal ions*, Trends in Analytical Chemistry, Vol. XXIX−7 (2010) 718−727.

[2] K. J. Kalbunde, Nanoscale Materials in Chemistry, Wiley, New York, USA, 2001.

[3] X. Ren, et al., *Carbon nanotubes as adsorbents in environmental pollution management: A review*, Chemical Engineering Journal, Vol. CLXX−2−3 (2011) 395–410.

[4] S. S. Andreescu, et al., *JEM Spotlight: Applications of advanced nanomaterials for environmental monitoring*, Journal of Environmental Monitoring, Vol XI−1 (2009) 27−40.

[5] M. Trojanowicz, *Analytical Applications of carbon nanotubes: a review*, Trends in Analytical Chemistry, Vol. XXV−5 (2006) 480−489.

[6] G. P. Rao, et al., *Sorption of divalent metal ions from aqueous solution by carbon nanotubes: A review*, Separation and Purification Technology, Vol. LVIII−1 (2007) 224−231.

[7] D. A. Britz and A. N. Khlobystov, *Noncovalent interactions of molecules with single walled carbon nanotubes*, Chemical Society Reviews, Vol. XXXV−7 (2006) 637–659.

[8] E .T. Thostenson, et al., *Advances in the science and technology of carbon nanotubes and their composites: a review*, Composites Science and Technology, Vol. LXI−13 (2001) 1899–1912.

[9] S. Agnihotri, et al., *Theoretical and experimental investigation of morphology and temperature effects on adsorption of organic vapors in single-walled carbon nanotubes*, Journal of Physical Chemistry B, Vol. CX−15 (2006) 7640–7647.

[10] J. V. Pearce, et al., *One-dimensional and two-dimensional quantum systems on carbon nanotube bundles*, Physical Review Letters, Vol. XCV−18 (2005) 185302.

[11] J. W. Jiang, et al., *Adsorption and separation of linear and branched alkanes on carbon nanotube bundles from configurational-bias Monte Carlo simulation*, Physical Review B, Vol. LXXII−4−5 (2005) 045447.

[12] C. Lu, F et al., *Surface modification of carbon nanotubes for enhancing BTEX adsorption from aqueous solutions*, Applied Surface Science, Vol. CCLIV−21(2008) 7035–7041.

[13] B. Lalović, et al., *Solid-phase extraction of multi-class pharmaceuticals from environmental water samples onto modified multi-walled carbon nanotubes followed by LC-MS/MS*, Environmental Science and Pollution Research, Vol. XXIV−25 (2017) 20784–20793.

[14] P. X. Hou, et al., *Purification of carbon nanotubes*, Carbon, Vol. XLVI−15 (2008) 2003−2025.

[15] F. F. Avilés, et al., *Evaluation of mild acid oxidation treatments for MWCNT functionalization*, Carbon, Vol. XLVII−13 (2009) 2970−2975.

[16] K. Pyrzynska, et al., *Application of solid phase extraction procedures for rare earth elements determination in environmental samples*, Talanta, Vol. CLIV (2016) 15−22.

[17] P. Verplank, et al., *Standard reference water samples for rare earth element determinations*, Applied Geochemistry, Vol. XVI−2 (2001) 231−244.

[18] S. Patra, et al., *Removal and Recycling of Precious Rare Earth Element from Wastewater Samples Using Imprinted Magnetic Ordered Mesoporous Carbon*, ACS Sustainable Chemistry & Engineering, Vol. V (2017) 6910−6923.

[19] M. Humphries, *Rare Earth Elements: The Global Supply Chain; CRS Report for Congress R41347*, Congressional Research Service: Washington, DC, 2011 http://web.mit.edu/12.000/www/m2016/pdf/R41347.pdf (accessed 08/06/2018).

[20] J. Florek, et al., *Functionalization of Mesoporous Materials for Lanthanide and Actinide Extraction*, Dalton Transactions, Vol. XLV−38 (2016) 14832−14854.

[21] N. Curtis, *Rare earths, we can touch them everyday*., "Lynas Presentation at the JP Morgan Australia Corporate Access Days", New York, 2010.

[22] K. Binnemans, et al., *Recycling of rare earths: a critical review*, Journal of Cleaner Production, Vol. LI (2013) 1−22.

[23] D. Carpenter, et al., *Uptake and Effects of Six Rare Earth Elements (REEs) on Selected Native and Crop Species Growing in Contaminated Soils*, PLoS ONE, Vol. X−6 (2015) e0129936. https://doi.org/10.1371/journal.pone.0129936

[24] S. Kulaksiz and M. Bau, *Anthropogenic gadolinium as a microcontaminant in tap water used as drinking water in urban areas and megacities*, Applied Geochemistry, Vol. XXVI−11 (2011) 1877–1895.

[25] https://www.nuclear-power.net/glossary/gadolinium (accessed 08/06/2018)

[26] J. C. Chow, et al., Nuclear data and the effect of gadolinium in the moderator, *AECL Nuclear Review*, Vol. I−1 (2012) 21−25.

[27] K. Kümmerer and E. Helmers, *Hospital Effluents as a Source of Gadolinium in the Aquatic Environment*, Environmental Science & Technology, Vol. XXXIV−4 (2000) 573−577.

[28] E. Kanal and M.F. Tweedle, *Residual or Retained Gadolinium: Practical Implications for Radiologists and Our Patients*, Radiology, Vol. CCLXXV−3 (2015) 630−634.

[29] U.S. Department of Energy. *Critical Materials Strategy*, https://energy.gov/sites/prod/files/DOE_CMS2011_FINAL_Full.pdf (accessed 08/06/2018)

[30] E. Alonso, et al., *Evaluating Rare Earth Element Availability: A Case with Revolutionary Demand from Clean Technologies*, Environmental Science & Technology, Vol. XLVI−6 (2012) 3406−3414.

[31] G. X. Xu, Rare Earth, Metallurgy Industry Press, Beijing, 1996.

[32] J. Z. Ni, Bio-Inorganic Chemistry of Rare Earth, Science Press, Beijing, 1995.

[33] E. Sabbioni, et al., *Longterm occupational risk of rare-earth pneumoconiosis: a case report as investigated by neutron activation analysis*, Science of the Total Environment, Vol. XXVI−1 (1982) 19–32.

[34] P. Liang, et al., *Determination of trace rare earth elements by inductively coupled plasma atomic emission spectrometry after preconcentration with multiwalled carbon nanotubes*, Spectrochimica Acta Part B: Atomic Spectroscopy, Vol. LX−1 (2005) 125–129.

[35] F. G. Shellock and A. Spinazzi, *MRI Safety Update 2008: Part 1, MRI Contrast Agents and Nephrogenic Systemic Fibrosis*, American Journal of Roentgenology, Vol. CXCI−4 (2008) 1129−1139.

[36] J. Künnemeyer, et al., *Speciation analysis of gadolinium-based MRI contrast agents in blood plasma by hydrophilic interaction chromatography/electrospray mass spectrometry*, Analytical Chemistry, Vol. LXXX−21 (2008) 8163–8170.

[37] C. L. Kahakachchi and D .A. Moore, *Identification and characterization of gadolinium(III) complexes in biological tissue extracts*, Metallomics, Vol. II−7 (2010) 490–497.

[38] S. Hao, et al., *The effects of chemical species on bioaccumulation of rare earth elements in wheat grown in nutrient solution*, Chemosphere, Vol. XXXV−8 (1997) 1699–1707.

[39] B. Nowack, et al., *Critical assessment of chelant-enhanced Metal Phytoextraction*, Environmental Science & Technology, Vol. XL−17 (2006) 5225–5232.

[40] R. Falter and R.-D. Wilken, *Determination of Rare Earth Elements by ICP- MS and Ultrasonic Nebulization in Sludges of Water*

Treatment Facilities, Vom Wasser, Vol. XC (1998) 57−64.

[41] M. F. Tweedle, K. Kumar, *Magnetic resonance imgaging (MRI) contrast agents*, *Metallopharmaceuticals II. Diagnosis and Therapie*, Springer: Berlin Heidelberg, New York 1999, p 23.

[42] A. H. El-Sheikh, et al., *Solid phase extraction and uptake properties of multi-walled carbon nanotubes of different dimensions towards some nitro-phenols and chloro-phenols from water*, International journal of environmental analytical chemistry, Vol. XCII−2 (2012) 190–209.

[43] A. Stafiej and K. Pyrzynska, Adsorption of heavy metal ions with carbon nanotubes, Separation and Purification Technology, Vol. LVIII (2007) 49–52.

[44] K. Pillay, et al., *Multi-walled carbon nanotubes as adsorbents for the removal of parts per billion levels of hexavalent chromium from aqueous solution*, Journal of Hazardous Materials, Vol. CLXVI (2009) 1067–1075.

[45] Z. Gao, et al., *Investigation of factors affecting adsorption of transition metals on oxidized carbon nanotubes*, Journal of Hazardous Materials, Vol. CLXVII−1−3 (2009) 357–365.

[46] D .A. Dzombak and F. M. M. Morel, *Surface complexation modeling*, in: Hydrous Ferric Oxide, Wiley, New York, NY, 1990.

[47] D. Mohan and K. P. Singh, *Single- and multi-component adsorption of cadmium and zinc using activated carbon derived from bagasse--an agricultural waste*, Water Research, Vol. XXXVI−9 (2002) 2304–2318.

[48] J. L. Barnhardt, et al., *Biodistribution of $GdCl_3$ and Gd-DTPA and their influence on proton magnetic relaxation in rat tissues*, Magnetic Resonance Imaging, Vol. V−3 (1987) 221–231.

[48] Y. S. Ho, G. McKay, *Application of Kinetic Models to the Sorption of Copper(II) on to Peat*, Adsorption Science & Technology, Vol. XX−8 (2002) 797–815.

[49] J. Febrianto, et al., *Equilibrium and kinetic studies in adsorption of heavy metals using biosorbent: A summary of recent studies*, Journal of Hazardous Materials, Vol. CLXII−2−3 (2009) 616−645.

[50] Y.S. Ho and G. McKay, *A comparison of chemisorption kinetic models applied to pollutant removal on various sorbents*, Process safety and environmental protection transactions of the Institution of Chemical Engineers, Part B., Vol. LXXVI−4 (1998) 332−340.

[51] Y. S. Ho, *Review of second-order models for adsorption systems*, Journal of Hazardous Materials, Vol. CXXXVI−3 (2006) 681−689.

[52] Y. S. Ho, et al., *Equilibrium isotherm studies for the sorption of divalent metal ions onto peat: copper, nickel and lead single component systems*, Water Air and Soil Pollution, Vol. CXLI−1−4 (2002) 1−33.

[53] E. Pehlivan, S. Cetin, *Sorption of Cr(VI) ions on two Lewatit-anion exchange resins and their quantitative determination using UV-visible spectrophotometer*, Journal of Hazardous Materials, Vol. CLXIII−1 (2009) 448−453.

[54] I. J. Langmuir, *The adsorption of gases on plane surfaces of glass, mica and platinum*, Journal of the American Chemical Society, Vol. XL−9 (1918) 1361−1403.

[55] A. S. Özcan and A. Özcan, Adsorption of acid dyes from aqueous solutions onto acid-activated bentonite, The Journal of Colloid and Interface Science, Vol. CCLXXVI−1 (2004) 39–46.

[56] H. M. F. Freundlich, *Over the adsorption in solution*, Journal of Physical Chemistry, Vol. LVII (1906) 385−470.

[57] J. Q. Jiang, et al., *Comparison of modified montmorillonite adsorbents. Part I: preparation, characterization and phenol adsorption*, Chemosphere XLVII (2002) 711−716.

[58] F.-C. Wu, et al., *A new linear form analysis of Redlich–Peterson isotherm equation for the adsorptions of dyes*, Chemical Engineering Journal, Vol. CLXII−1 (2010) 21–27.

[59] H. Shahbeig, et al., *A new adsorption isotherm model of aqueous solutions on granular activated carbon*, World Journal of Modelling and Simulation, Vol. IX−4 (2013) 243−254.

ꕥ

СОРПЦИЈА ГАДОЛИНИЈУМА НА ВИШЕСЛОЈНИМ УГЉЕНИЧНИМ НАНОТУБАМА

Сажетак: Ретке земље се сматрају материјалима будућности захваљујући својим бројним применама, у које спадају медицинска дијагностика, нуклеарна постројења, нафтна индустрија, итд. Вишеслојне угљеничне нанотубе, које имају јединствена физичко-хемијска својства, у овом раду су испитане као сорбенти лантаноида гадолинијума из водених раствора. Зависност сорпције Gd од pH

испитивана је у опсегу pH 3–11 на собној температури (298 K). Равнотежна сорпција у опсегу почетних концентрација 5–50 mg L^{-1} анализирана је Лангмировим, Фројндлиховим и Редлих–Петерсоновим моделима. Кинетика сорпције анализирана је моделима псеудопрвог реда, псеудодругог реда и фракционог степена.

Кључне речи: гадолинијум, вишеслојне угљеничне нанотубе, сорпција.

Paper received: 22 August 2018
Paper accepted: 15 February 2019